JOURNAL OF PROPULSION AND POWER
Vol. 18, No. 3, May–June 2002

Shape Optimization of Supersonic Turbines Using Global Approximation Methods

Nilay Papila* and Wei Shyy†
University of Florida, Gainesville, Florida 32611-6250
and
Lisa Griffin‡ and Daniel J. Dorney§
NASA Marshall Flight Center, Huntsville, Alabama 35812

There is growing interest to adopt supersonic turbines for rocket propulsion. However, this technology has not been actively investigated in the United States for the last three decades. To aid design improvement, a global optimization framework combining the radial-basis neural network (NN) and the polynomial response surface (RS) method is constructed for shape optimization of a two-stage supersonic turbine, involving $\mathcal{O}(10)$ design variables. The design of the experiment approach is adopted to reduce the data size needed by the optimization task. The combined NN and RS techniques are employed. A major merit of the RS approach is that it enables one to revise the design space to perform multiple optimization cycles. This benefit is realized when an optimal design approaches the boundary of a predefined design space. Furthermore, by inspecting the influence of each design variable, one can also gain insight into the existence of multiple design choices and select the optimum design based on other factors such as stress and materials consideration.

Nomenclature

h	=	basis functions
W	=	total weight of the turbine
w	=	coefficients of the linear combinations or weights
Δpay	=	payload increment
η_{t-s}	=	total to static efficiency
η_{t-t}	=	total to total efficiency

Introduction

TURBINE performance directly affects engine specific impulse, thrust-to-weight ratio, and reliability in a rocket propulsion system. In the last three decades, supersonic turbines have not been designed for rocket propulsion in the United States. There is growing interest to reconsider this technology for space transport. Designing a multistage turbine is a labor-intensive task because of the substantial number of variables involved in the problem. Clearly, a formal optimization methodology will be valuable to help meet the design goals by maximizing the performance objective while addressing the structures and materials considerations. A number of papers, using approaches such as sensitivity evaluations,[1–5] genetic algorithms,[6–8] or response surface methods (RSMs),[9–12] have been published in this area. In this work, a global optimization methodology, based on the radial-basis neural networks (RBNN) and the polynomial-based RSM under development,[13,14] is employed to facilitate design optimization for supersonic turbines intended for reusable launch vehicle (RLV) applications.

We select the use of the global optimization technique because it has several advantages[15]: 1) Calculation of the local sensitivity of each design variable is not required. 2) Information collected from various sources and by different tools can be utilized. 3) Multi-criterion optimization is offered. 4) The existence of multiple design points and tradeoffs can be handled. 5) Tasks may be easily performed in parallel. 6) The noise intrinsic to numerical and experimental data can often be effectively filtered. Approximations techniques are critical to the optimization procedure. Among alternative global approximation techniques, the RSM has gained the most attention due to its flexibility in handling different types of information.[16] The RSM expresses the objective and the constraint by simple functions, often polynomials, which are fitted to the selected points. One can use RBNN-based and polynomial-based RSM techniques to model the relationship between design variables and objective/constraint functions of the overall approach. In the present work, the RBNN is employed to supply additional data to help construct improved polynomial representation of the response surface (RS). In other words, RBNN feeds data into polynomials before the optimization task is conducted. Such a practice has been shown to be beneficial[12–14] and can help to assess the adequacy of the RS model when there is insufficient amount of information available.

With the aid of the global optimization technique, both preliminary and detailed shape designs of a supersonic turbine are considered. The main purpose for preliminary optimization is to determine the optimum configuration in terms of the number of stages, sizing, revolutions per minute, and compatibility between operating variables, as reported in Ref. 17. Based on these findings, shape optimization is conducted for each vane and blade, based on the Navier–Stokes computational fluid dynamics (CFD) simulations.

In any optimization process, especially with global optimization techniques, the amount and the distribution of data required is a critical issue. To help address this question, we have investigated the issues related to the design of experiments (DOE). Typically, the face-centered composite design (FCCD)[18] is employed. This approach can be quite costly as the number of design variables increases. Additional criteria can be established to help improve the efficiency and effectiveness of the construction of the RS by employing the concept of orthogonal arrays (OA)[19] and d-optimality.[20] These methods will be discussed in the following sections.

Presented as Paper 2001-1065 at the AIAA 39th Aerospace Sciences Meeting and Exhibit, Reno, NV, 8–11 January 2001; received 27 March 2001; revision received 18 December 2001; accepted for publication 26 December 2001.

*Graduate Student, Department of Aerospace Engineering, Mechanics and Engineering Science. Student Member AIAA.
†Professor and Chair, Department of Aerospace Engineering, Mechanics and Engineering Science. Fellow AIAA.
‡Engineer, Space Transportation Directorate. Member AIAA.
§Engineer, Space Transportation Directorate. Associate Fellow AIAA.

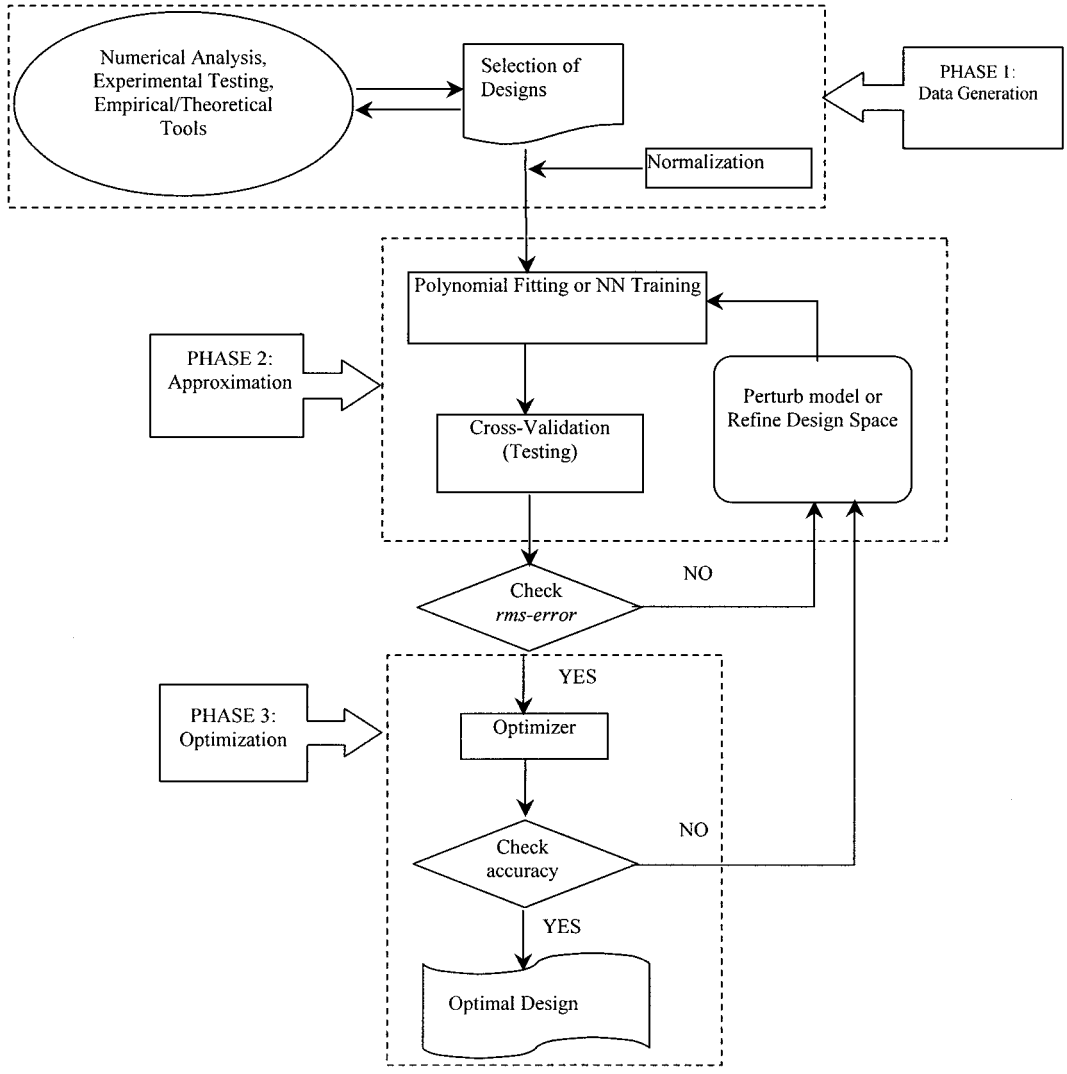

Fig. 1 Schematic of the RS based optimization procedure.

Approach

As shown in Fig. 1, the entire optimization process can be divided into three parts: 1) data generation, 2) polynomial- or NN-generation phase for establishing an approximation, and 3) optimizer phase. In the first phase, the representation of design space is decided. In the second phase, polynomials or NN (or combined) models are generated with the available training data set. Finally, in the third phase, the optimizer uses the polynomial or NN approximations during the search for the optimum until the final converged solution is obtained.

The optimization technique follows previous works for optimizing fluid machinery, such as diffuser, injector, and airfoil, as presented in Refs. 13–15, 17, and 21–23. The NN technique and the polynomial RSM are integrated to offer enhanced optimization capabilities by Shyy et al.[14] Optimization of a supersonic turbine for preliminary design, using the polynomial RSM, is presented by Papila et al.[17] Papila et al.[21] investigated the effect of data size and relative merits between polynomial and NN-based RSM in handling varying data characteristics. Issues related to numerical noises and the interaction between CFD models and RSM are addressed by Madsen et al.[22] Tucker et al.[23] made a first effort to apply RSM for injector optimization. In Refs. 13 and 14 a comprehensive update of the concepts and applications of the global optimization method is offered, including the mentioned examples.

Overview of the RS Literature

Polynomial-based RS techniques are attractive because finding the polynomial coefficients is a linear regression process. The linearity decreases the computational cost and provides an advantage when the simulations have substantial amount of numerical noise. However, one can also design a linear NN model. The RBNN is such an example. In terms of the ability of filtering noise from experimental data, polynomial-based RSM has certain advantages over NNs. However, if the number of neurons used to design the NN is not the same as the data, then, by definition, filtering is also performed by the NN. When it comes to handling complex functions, NN are more flexible to fit complex functions. This advantage is particularly noticeable if the level of numerical noise is low.

A growing number of papers have been published to combine NN- and polynomial-based RSM approximations (for example, Refs. 11–14 and 24, 25). For example, the work done by Rai and Madavan,[11,24,25] Madavan et al.,[12] and Shyy et al.[14] suggests that NN can be effectively used to supplement the existing training data to help generate a more accurate polynomial. RBNN may lack satisfactory filtering properties in some cases, as stated by Papila et al.[21] and Vaidyanathan et al.[26] However, once trained, RBNN can generate additional design data easily to feed the polynomial-based RSM. This approach is also employed in this work.

RBNN

NN are massively parallel computational systems comprising simple nonlinear processing elements with adjustable interconnections.[27,28] The predictive ability of the network is stored in the interunit connection strengths called weights obtained by a process of adaptation to, or learning from, a set of training patterns.

Training of a network requires repeated cycling through the data and continues until the error target is met or until the maximum number of neurons is reached. This paper focuses on RBNN, which is a multilayer network with hidden layers of radial-basis function and a linear output layer. Radial-basis functions (RBF) are activation functions for which the response decreases or increases monotonically with distance between the input and the RBF's center. The distance between two points is determined by the difference of their coordinates and by a set of parameters.[29]

A main advantage of the RBNN approach is the ability to reduce the computational cost due to the linear nature of RBNN.[30] An RBNN is a linear model because the basis functions h, in Eq. (1), and any parameters, which they might contain, are fixed through the training process:

$$f(x) = \sum_{j=1}^{m} w_j h_j(x) \tag{1}$$

where w are the coefficients of the linear combinations or weights.

For linear RBNN models, a least-squares principle that minimizes the sum-squared errors can be applied for training, and then m unknown weights can be solved based on the mean square error of the training set. However, the criterion of the mean square error of the training set is unlikely to achieve reasonable results for predicting the unknown input. For this purpose, test data should be used when selecting the model. This is the basic form of cross validation.[29,30] In this study, the RBNN model is designed by using the functions developed by Orr[29–31] for MATLAB®.[32] Among several choices given by Orr,[29] the RBNN method based on ridge regression[30] is used because it can optimize the RBF widths to improve the data fitting capability. To choose between competing models, the maximum marginal likelihood method[31] is used as a model selection criterion.

Polynomial-Based RS Techniques

The polynomial-based RSM models the system with assumed order and unknown coefficients. The solution for the set of coefficients that best fits the training data is a linear least-square problem,[18] and so it is computationally straightforward. The linearity also allows us to use statistical techniques such as DOE to find efficient training sets. Statistical techniques are also available for identifying polynomial coefficients that are not well characterized by the data. These coefficients are discarded to improve the predictive capability of the polynomial. Finally, these statistical tools allow us to estimate the error of the polynomial-based model at points not used for training, that is, its prediction error.

In this study, the RSs are generated by standard least-squares regression using JMP, a statistical analysis software with a variety of statistical analyses functions in an interactive manner.[33] The global fit and prediction accuracies of the RSs are assessed through statistical measures such as the coefficient of multiple determination (R^2), its adjusted value to account for the degrees of freedom in the model (R^2_{adj}), and the rms-error variation.

DOE

To minimize the effect of the noise on the fitted polynomial and NN, and to improve the representation of the design space, the DOE procedure can be used to select the data to be used in construction of the RSs or training of the RBNN. There are a number of different designs of experiment techniques in the literature, as reviewed in Ref. 34. Issues related to our approach are reviewed in Ref. 17 and will not be repeated here. In this study, FCCD, OA, and d-optimal design methods are used to select the effective design space. The FCCD is widely used for fitting second-order RSs.[18] It selects design points at the corners of the design space, center of the faces, and the center of the design space. Therefore, FCCD yields $2^N + 2N + 1$ points, where N is the number of design variables. On the other hand, an OA is a fractional factorial matrix that assures a balanced comparison of levels of any factor or interaction of factors.[19] Because the points are not necessarily at vertices, OA tools can be more robust than the FCCD. Based on the design of experiment theory, OA can significantly reduce the number of experimental configurations.[17] Finally, the d-optimal design minimizes the generalized variance of the estimates that is equivalent to maximizing the determinant of the moment matrix.[18] The d-optimal design approach makes use of the knowledge of the properties of the polynomial model in selecting the design points. This criterion tends to emphasize the parameters with the highest sensitivity.[34]

Optimization Procedure

The focus in the present work is the interplay between the number of design variables and the predictive capability and input requirement of the RSM. Microsoft Excel SOLVER[35] is used as an optimization toolbox together with the polynomial RS technique throughout the work. SOLVER applies the generalized reduced gradient optimization method to find the maximum or minimum of a function with given constraints.[36]

Results and Discussion

Preliminary Design

For preliminary design, we have considered single-, two-, and three-stage turbines with the number of design variables increasing from 6 to 11 then to 15, in accordance with the number of stages. The preliminary design data are obtained by using the computer code MEANLINE.[37] The MEANLINE code performs one-dimensional analyses that employ loss correlations gleaned from experimental databases. It predicts performance, calculates gas conditions and velocity triangles, generates a flowpath elevation, and estimates the turbopump weight. It also provides an initial spanwise distribution of row exit angles based on the assumption of constant axial velocity and conservation of radial momentum.

The optimum preliminary design is obtained by using polynomial-based RSM coupled with a MEANLINE analysis. The results indicate that the two-stage turbine gives the best performance based on the combined measures between efficiency and weight. This configuration is adopted for detailed vane (stator) and blade (rotor) shape optimization.

Detailed Shape Design

In detailed design, the shapes of the vanes and blades are generated. To generate optimum detailed designs, CFD analysis, RBNN, and polynomial-based RSM are used. Ideally, the detailed optimization would be conducted to have both stages, in three dimensions, optimized simultaneously. However, the sheer number of design variables made this approach impractical. Therefore, first the mean airfoil contours of each component are optimized. Airfoil contours are generated using a geometry generator developed for this task that could read a matrix of design variables, generate and plot the airfoil, and write a preliminary input file for the CFD grid generator.[37] Because a substantial portion of the loss in a supersonic turbine can be attributed to interactions between the first two rows, unsteady CFD calculations are performed for the first stage, running parametrics on the vane first with the baseline blade, and then performing the blade parametrics with an optimized vane. For detailed design, CFD calculations are performed using WILDCAT, a parallelized, unsteady, quasi-three-dimensional Navier–Stokes code that utilizes moving grids to simulate the rotor motion.[6,37,38]

First Vane

There are seven design variables for detailed design of the first vane. These are leading edge (LE) pressure side height/axial chord H/L, uncovered turning (UT), and Bezier curve control handles, $L1$, $L3F$, $L3R$, $L4$, and $L5$. The design variable ranges are selected for the design optimization; they are decided in consultation with industry colleagues with strong expertise in the area (see Acknowledgment). For this case, FCCD yields 143 possible design points. After the addition of six more levels, as shown Fig. 2, 437 design points are obtained. The d optimality for a reduced cubic model with 40 coefficients is used to decrease the data size to half. However, some of these designs have resulted in negative thickness. Consequently, 203 CFD solutions are generated for RS model construction.

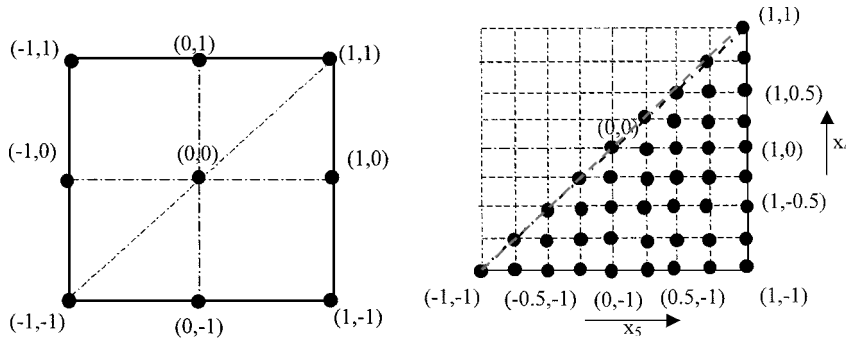

Fig. 2 Design of experiment for the first vane.

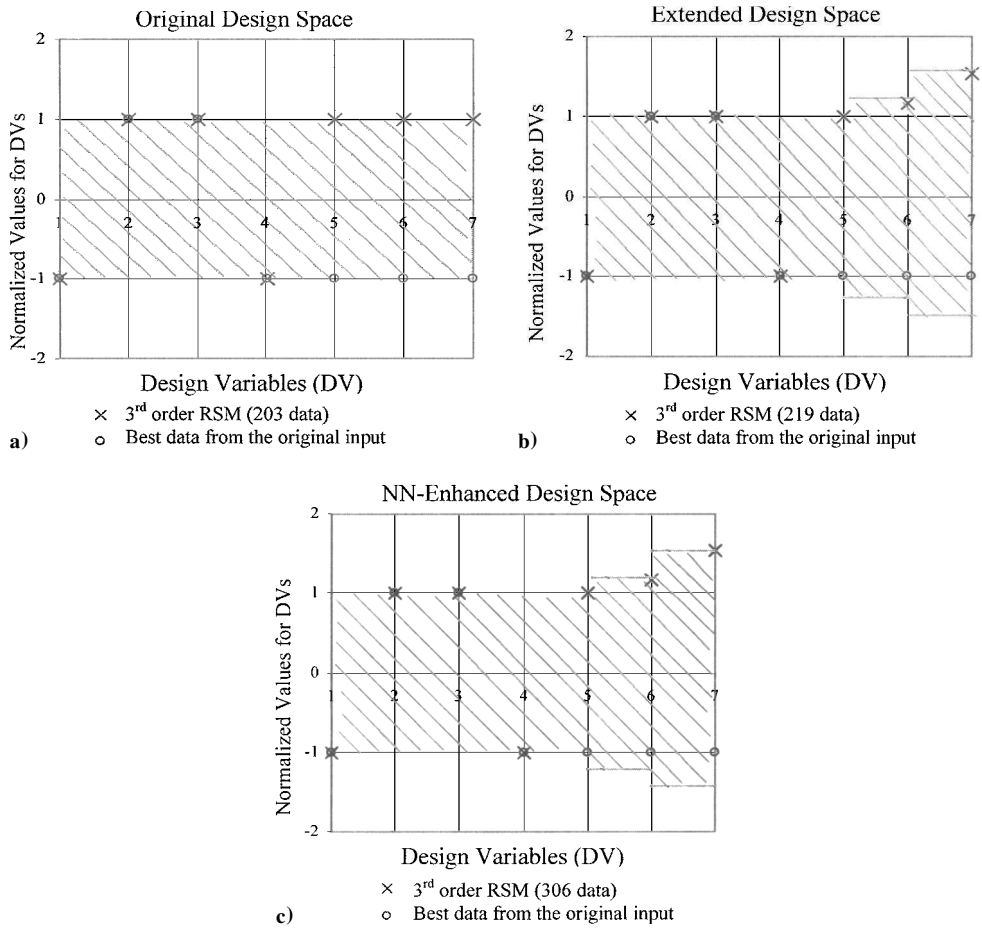

Fig. 3 Comparison of the optimum design variables (DV) for the first vane: a) original design space (cycle 1), where the design variables are bounded between − 1 and +1, b) extended design space (cycle 2), and c) NN-enhanced design space (cycle 3).

The objective for detailed design optimization is the stage total-to-total efficiency, η_{t-t}. The minimum thickness that should be greater or equal to 0.055 is the only design constraint of the first vane optimization.

A three-cycle optimization strategy has been adopted for the first vane. The statistical summary of the RS models resulting from the three cycles is shown in Table 1. In cycle 1, we have employed the stepwise regression method to create a reduced cubic polynomial model, with 40 coefficients, to identify the optimal design points. The design variables corresponding to the optimized vane shape are shown in Fig. 3. Note that the optimum design approaches the boundary of the design space. Naturally, it seems fruitful to consider expanding the design space to further improve the design by generating additional information in an extended region. Accordingly, in cycle 2, the design space is modified by extending the ranges of two design variables, namely, $L4$ and $L5$. As shown in Table 2, 16 new data points are added to the database. The reduced cubic polynomial RS is again constructed based on the extended design space.

In cycle 3, a technique based on the NN-enhanced RSM is developed. The procedures can be summarized as follows:

1) RBNN is constructed for the subset of 177 points from the 203 data points from cycle 1 and is tested by using the rest of the 26 data points.

2) The trained RBNN is used to predict 87 additional data points (50 OA data points plus 37 previously excluded FCCD data). These data are added to the existing data set of 219 points used in cycle 2.

3) In cycle 3, with the enhanced data, the reduced cubic polynomial RS is constructed and tested by using the same 26 data points.

4) The optimum design is determined for the enhanced design space in cycle 3.

The results of the optimal designs from all cycles and the CFD results for cycles 2 and 3 are summarized in Table 3. Note that the second and third optimization cycles converges to the same optimal design. Based on the diagnosis, for example, contour plots, it appears that the RS is quite flat with respect to certain design variables, for example, $L4$ and $L5$, in regions close to the optimal designs. Consequently, small deviations in other variables can cause noticeable shifts. However, there are multiple design points, including the best data point from the CFD runs, which offer essentially the same performance. This outcome means that other considerations such as stress distribution and manufacturing difficulties can be usefully incorporated into the final selection stage.

Figure 3 shows the comparison of the optimal design variables [normalized to $(-1, +1)$ range] for reduced cubic models for all design cycles. Figure 4 shows that the designs converge to the same configuration between cycles 2 and 3. On the other hand, as shown in Fig. 5, there are multiple design points that exhibit essentially the same performance (within the modeling uncertainty), albeit with much different geometries. To help better understand these observations, we assess the sensitivity of the two geometric variables ($L4$ and $L5$) in Fig. 6, which shows that the performance of the vane is very insensitive to $L5$. The two shapes shown in Fig. 5 are mainly caused by $L5$, which explains why two very different vane shapes give essentially the same performance. From the structural point of view, the value of $L5$ to produce a thicker profile is preferable. This example demonstrates that the global optimization technique enables one to compare designs based on insight into the entire design space, which allows a suitable selection to be made with additional factors considered.

Figure 7 shows the absolute Mach contours of the two vanes shown in Fig. 5. From Figs. 7a and 7b, observe that the first vane shape is optimized to a contour with the airfoil throat at the trailing edge and with no concave curvature on the suction side as opposed

Table 1 Quality the polynomial RS models for the original (cycle 1), extended (cycle 2) and NN-enhanced (cycle 3) design spaces for the first vane[a]

Head	Reduced cubic model, 203 data (cycle 1)	Reduced cubic model, 219 data (cycle 2)	Reduced cubic model, 306 data (cycle 3)
R^2	0.8	0.8	0.7
R^2_{adj}	0.8	0.8	0.7
rms-error, %	1.10	1.10	1.30
Observations (or sum weights)	203	219	306

[a]Mean of response is normalized by the baseline η_{t-t}.

Table 2 Comparison of the original (cycle 1), extended (cycle 2), and NN-enhanced (cycle 3) design spaces for the first vane

	Cycle 1		Cycle 2		Cycle 3	
Design variable	Lower limit	Upper limit	Lower limit	Upper limit	Lower limit	Upper limit
H/L	0.79	1.19	0.79	1.19	0.79	1.19
UT	−1.20	−0.20	−1.20	−0.20	−1.20	−0.20
$L1$	0.36	2.00	0.36	2.00	0.36	2.00
$L3$F	0.44	1.76	0.44	1.76	0.44	1.76
$L3$R	0.25	2.00	0.25	2.00	0.25	2.00
$L4$	0.05	1.25	0.01	1.35	0.01	1.35
$L5$	0.13	2.00	0.01	2.50	0.01	2.50

Table 3 Optimum designs for the original (cycle 1), extended (cycle 2), and NN-enhanced (cycle 3) design spaces for the first vane[a]

Variable	Original design space (cycle 1) 203 data	Extended design space (cycle 2) 219 data	NN-enhanced design space (cycle 3) 306 data
H/L	0.791	0.791	0.791
UT	0.2	0.2	0.2
$L1$	2	2	2
$L3$F	0.441	0.441	0.441
$L3$R	2	2	2
$L4$	1.25	1.35	1.35
$L5$	2	2.5	2.5
$\eta_{t-t\ RSM}$	1.042	1.044	1.043
$\eta_{t-t\ CFD}$	N/A	1.031	1.031

[a]All design variables and η_{t-t} are normalized by the baseline values.

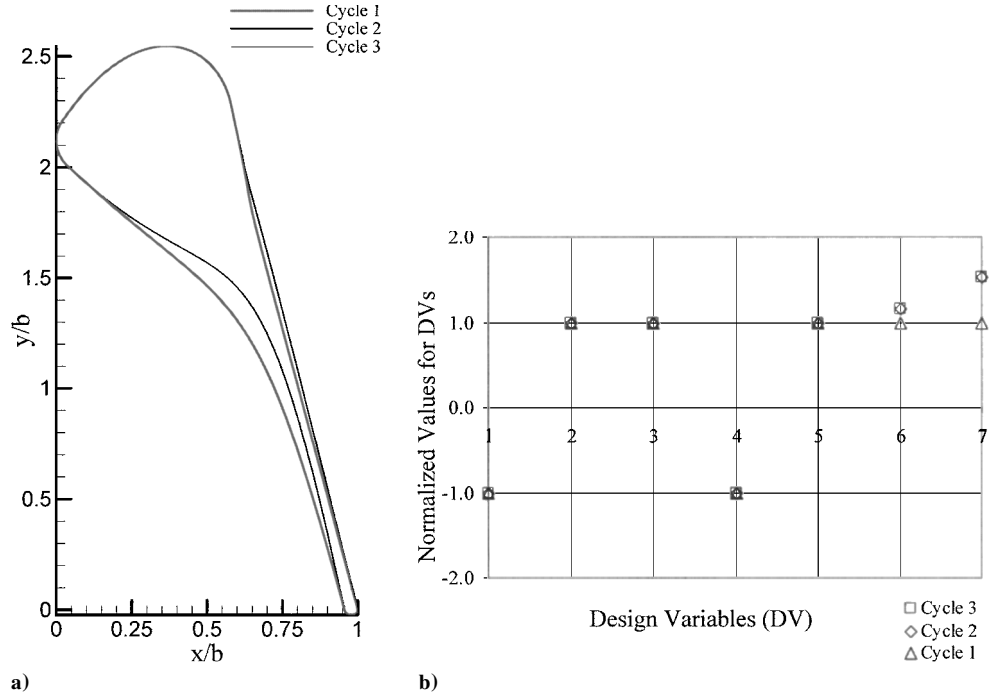

a) b)

Fig. 4 Summary of the three optimization cycles for the first vane: a) optimal cross sections (optimal designs of cycles 2 and 3 coincide because they converge to the same configuration) and b) optimum design variables (where − 1 and +1 show the minimum and maximum values of the design variables in the original design space, respectively).

to the more conventional supersonic vane. The optimized contour results in continued expansion and acceleration on the suction side downstream of the throat. This additional acceleration appears to reduce undesirable vane-to-blade interaction by attenuating the blade leading-edge shock sweeping across the aft portion of the vane suction side.[39]

First Blade

There are 11 design variables for detailed design of the first blade. These are LE pressure side height/axial chord H/L; LE metal angle β_1; UT; six different Bezier curve control handles, $L1$, $L2F$, $L3R$, $L4$, $L5$, and $L7$; channel convergence ratio (CCR); and the circle factor (CF). The ranges of the design variables are determined in consultation with industry colleagues with strong expertise in the area (see Acknowledgment). Again, the stage total-to-total efficiency η_{t-t} is selected as the objective function to be maximized for the blade design. For the first blade, three different constraints need be satisfied:

1) The minimum thickness should be greater or equal to trailing-edge diameter.

2) $L1 + L2F + (1.9 \times \text{CF})$ should be smaller than 2.7 because if this parameter is more than 2.7, the airfoil develops a kink in the suction side of the LE.

3) The suction side radius of curvature must be greater than five times that of the trailing-edge radius. This also helps to eliminate unrealistic airfoil shapes such as those with kinks.

For this case, a five-level OA-based procedure has been adopted to select 250 desgin points for the CFD code to generate solutions. A software tool developed by Owen[19] is used for constructing OA designs. Because these points are located at either the edge or the center of the design space, additional 23 FCDD data points at the center of the faces are added. Finally, 38 data points along the main diagonal of the design space is generated. In short, 311 possible design points are selected to generate the CFD solutions. However, only 139 out of the 250 OA selected data points, 21 out of the 23 FCCD selected data points, and 17 out of the 38 diagonal-baseddata points are obtained from the CFD tool. Therefore, only 177 possible design points, out of the 311 total, have been collected. The cases are not completed because the airfoil shapes are unrealistic, which cause either excessively high losses, or prevent the grid generation process from running appropriately. These nonphysical cases create holes in the design space, which cause difficulties in constructing RSs. Figure 8 shows the distribution of these holes within the design space. As one can see from Fig. 8, the difficulty is along the diagonal ends, as well as on the edges of the design space. With only 177 data points generated for 11 design variables, RBNN is used to produce additional information, as described in the following paragraphs.

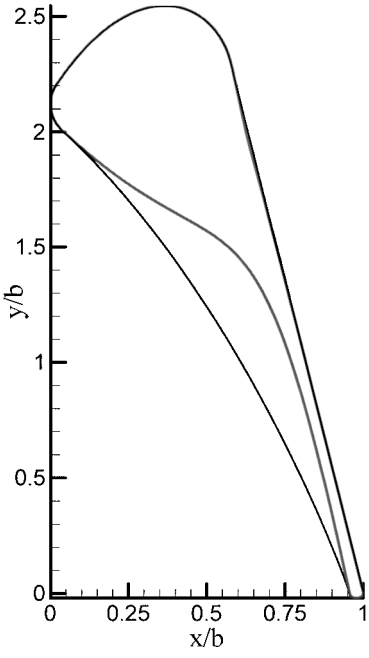

Fig. 5 Multiple possibilities for the first vane; both designs offer comparable efficiency, but the thicker profile is preferred from structural considerations.

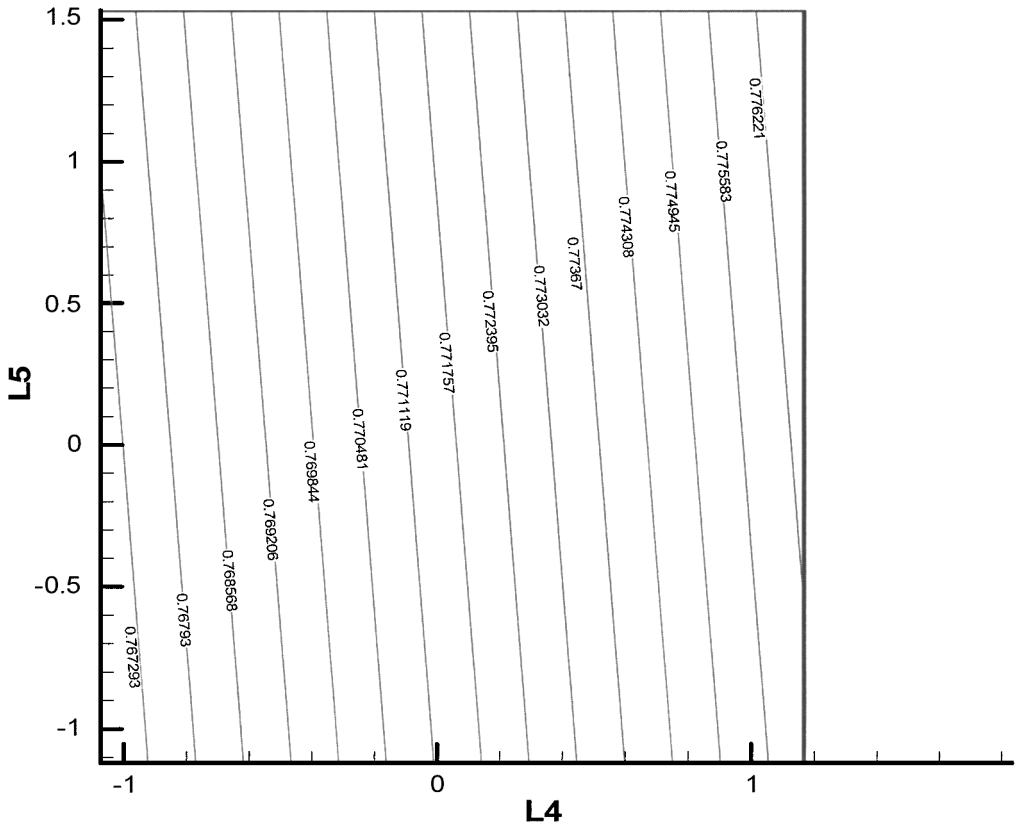

Fig. 6 Efficiency contours for 203 data of cycle 1, showing that *L5* has little impact on the performance of first vane.

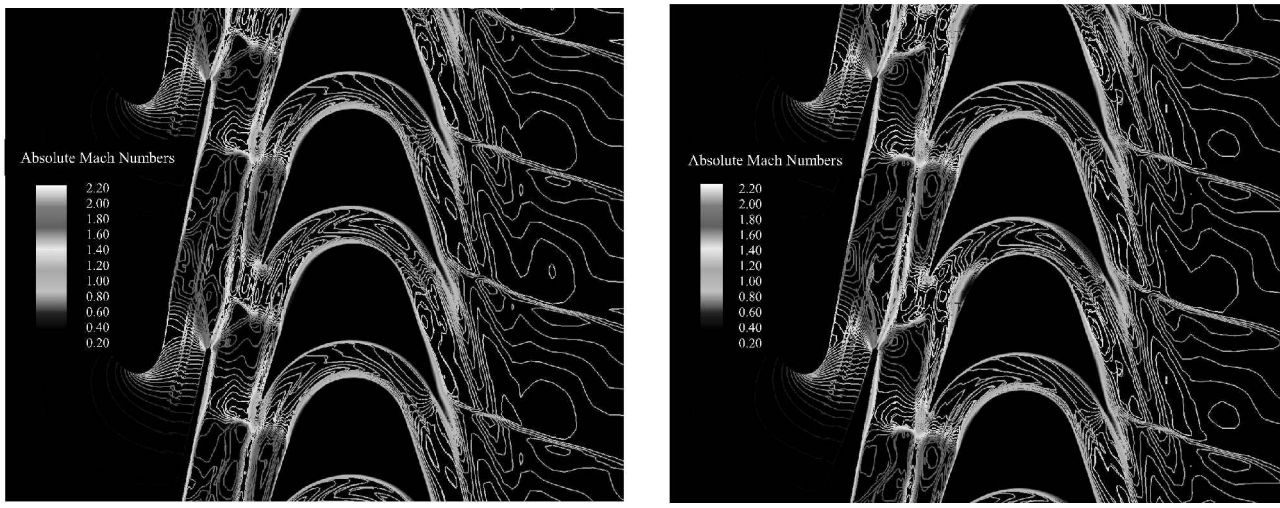

a) Baseline configuration **b) Optimum configuration**

Fig. 7 Instantaneous absolute Mach number contours for two first vane designs of essentially equal performances.

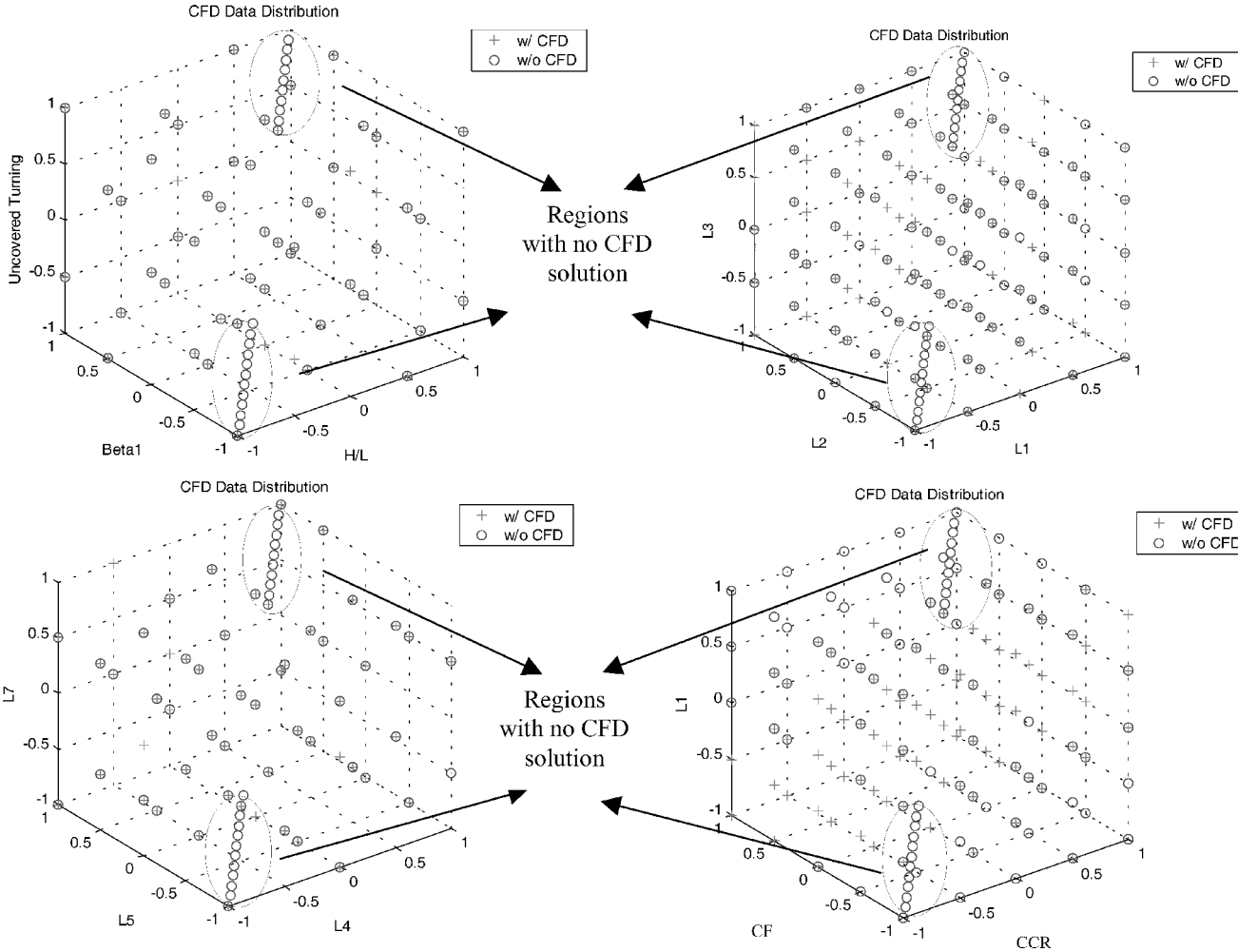

Fig. 8 Summary of the cases for both successful and unsuccessful CFD simulations for the first blade.

RBNN is trained based on the 160 data points from the mentioned 177 CFD-generated data points, with the remaining 17 points reserved to tune the configuration of the NNs.

The trained RBNN is used to generate additional 2204 design points. As shown in Fig. 9, 2070 of them are selected using FCCD data modified, and the remaining 134 of them are the cases for which CFD code does not converge.

Full quadratic and reduced cubic RS models are constructed for the first blade. A total of 38 data points are used to test both models of which 17 are from the CFD runs (originally selected as the test data) and 21 are from the NN-enhanced data. The statistical summary for both models, with and without NN-enhanced data, is shown in Table 4.

In the course of performing the optimization task, it is realized that out of the 11 design variables, 5 of them, responsible for the shape in the rear portion of the upper blade surface, can be optimized first because various plausible shapes converge to the similar values of them. Accordingly, one can reduce the design space from

Table 4 Quality of the polynomial RS model for the first blade

Summary of fit	Quadratic model without NN-data (plain CFD data), cycle 1	Quadratic model (NN-enhanced data), cycle 2	Reduced cubic model (NN-enhanced data), cycle 3
R^2	0.78	0.87	0.97
R^2_{Adj}	0.57	0.86	0.97
rms-error, %	3.82	1.74	0.81
Observations (or sum weights)	160	2343	2343

Table 5 Optimum cases for the first blade obtained by reduced cubic model with NN-enhanced data for modified variable ranges[a]

Variable	Blade-1	Blade-2
$\eta_{t-t\ RSM}$	1.04	1.07
$\eta_{t-t\ CFD}$	1.05	1.04
H/L	−25	−25
β_1	0.94	0.99
UT	0.63	0.63
$L1$	0.59	0.67
$L2F$	1.48	1.36
$L3R$	1.55	1.6
$L4$	0.68	0.68
$L5$	1.78	1.44
$L7$	0.66	0.76
CCR	1.06	1.06
CF	3.78	3.78

[a]All design variables and η_{t-t} are normalized by the baseline values.

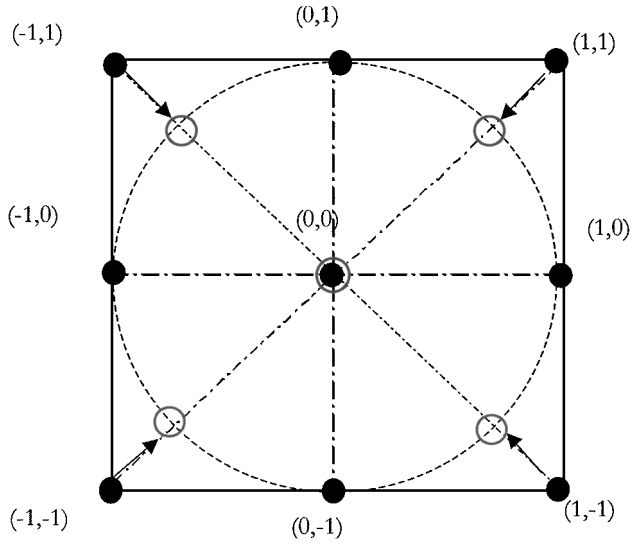

Fig. 9 Schematic of the additional data generated for the first blade in two dimensions: ●, is original FCCD and ○, is modified FCCD data to be added by NN.

11 to 6 variables. Two designs are presented with the five fixed design variables and different six variables, as shown in Table 5 and Fig. 10. With six design variables fixed, the two blade shapes yield very comparable performance. Their shapes in the upper rear portion are, as expected, virtually the same. On the other hand, their front portions are noticeably different, with blade 1 exhibiting more variations than blade 2. Again, with the insight offered by the global model, we have an opportunity to evaluate not only the sensitivity of each design variable, but also additional tradeoffs between comparable designs.

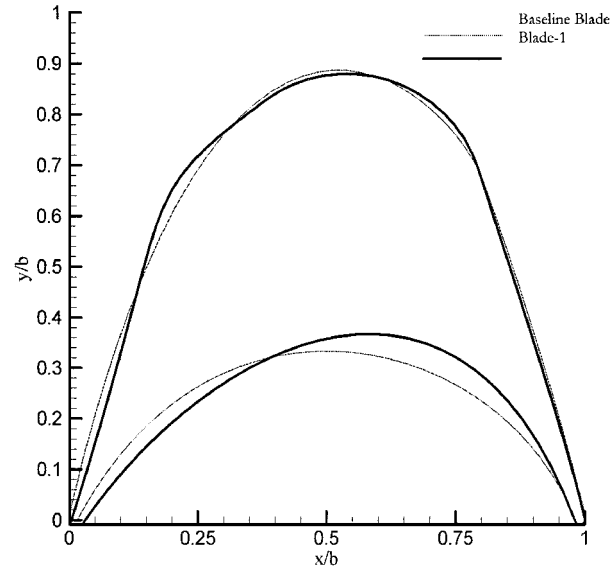

Blade 1

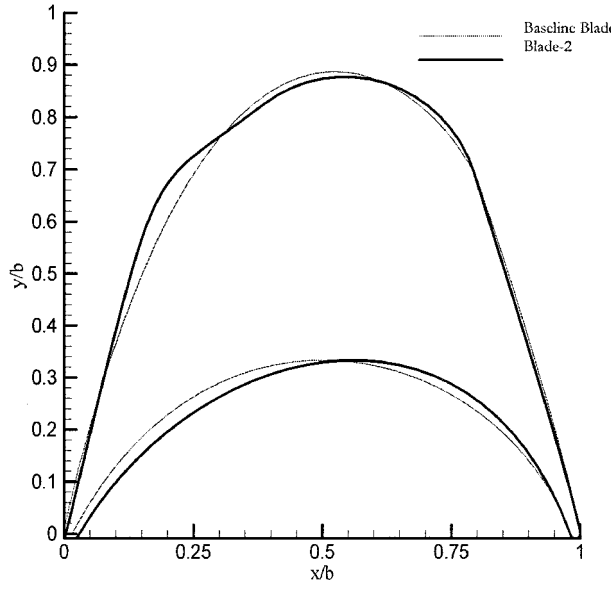

Blade 2

Fig. 10 Optimum shapes for the first blade obtained by reduced cubic model with NN-enhanced data for modified design variable ranges.

Conclusions

A methodology to improve the supersonic turbine performance has been developed for preliminary and detailed design. A global optimization framework combining the RBNN and the polynomial-based RSM is constructed. Based on the optimized preliminary design, shape optimization is performed for the first vane and blade of an optimized two-stage supersonic turbine. The results obtained can be summarized as follows.

1) The design of experiment approach is critical in reducing the data size needed by the optimization task.

2) A major merit of the global optimization approach is that it enables one to revise adaptively the design space to perform multiple optimization cycles.

3) As evidenced by the three optimization cycles conducted for the first vane, capabilities to refine adaptively the optimization scope and procedure can be critical when an optimal design approaches the boundary of a predefined design space. For the first blade, the optimization process indicates that 5 out of the 11 design variables can be chosen first, leaving the design space to reduce to have 6

variables. Based on the reduced set of design variables, the optimization task can be handled more effectively.

4) In the present study, the design variables and their ranges are selected in consultation with industry colleagues well experienced in the field. It is found that a number of cases create airfoil shapes that are unrealistic. Consequently, they either cause excessively high losses, or prevent the grid generation process from running appropriately. These nonphysical cases create holes in the design space, which cause difficulties in constructing RSs. The combined NN, RS techniques, and multiple optimization cycles help address these fundamental barriers.

5) By inspecting the influence of each design variable, one can also gain insight into the existence of multiple design choices and select the optimum design based on other factors such as stress and materials considerations.

6) NN-enhanced RSM helps to improve the accuracy of the RSM, useful for smoothing out the design space, and allows the optimization task to be conducted with smaller number of CFD runs, as illustrated in first blade example.

Note that the optimal shapes involve a substantial number of design variables at the limit of the assigned design space. This situation did not happen because of the lack of experience; the design space was defined in direct consultation with the colleagues from rocket propulsion industry (see Acknowledgment). For new technologies, it is not unusual that our initial judgment needs to be refined, as is the case here. In such situations, the capability of assessing the characteristics of the entire design space is critically important. The other side of the coin is that, to perform such optimization tasks with confidence, one needs to be able to estimate the fidelity of the RS model. In addition to the information presented here, the relevant issues have been addressed in Refs. 22, 40, and 41, which may be consulted.

Acknowledgments

This work has been supported by NASA Marshall Space Flight Center. We appreciate the useful discussions with F. Huber, Riverbend Design Services, Palm Beach Gardens, Florida (private communication, February 2000) and K. Tran, The Boeing Company, Rocketdyne, Canoga Park, California (private communication, February 2000).

References

[1]Lee, S.-Y., and Kim, K.-Y., "Design Optimization of Axial Flow Compressor Blades with Three-Dimensional Navier–Stokes Solver," American Society of Mechanical Engineers, ASME Paper 2000-GT-0488, May 2000.

[2]Baysal, O., and Ghayour, K., "Continuous Adjoint Sensitivities for General Cost Functionals on Unstructured Meshes in Aerodynamic Shape Optimization," AIAA Paper 98-4904, Sept. 1998.

[3]Sørensen, D. N., Thompson, M. C., and Sørensen, J. N., "Toward Improved Rotor-Only Axial Fans—Part II: Design Optimization for Maximum Efficiency," *Journal of Fluids Engineering*, Vol. 122, No. 2, 2000, pp. 324–329.

[4]Janus, J. M., and Newman, J. C., III, "Aerodynamic and Thermal Design Optimization for Turbine Airfoils," AIAA 2000-0840, Jan. 2000.

[5]Yiu, K. F. C., and Zangeneh, M., "Three-Dimensional Automatic Optimization Method for Turbomachinery Blade Design," *Journal of Propulsion and Power*, Vol. 16, No. 6, 2000, pp. 1174–1181.

[6]Snodgrass, R., Dorney, D. J., Sandgren, E., and Merz, L. F., "Multiobjective Shape Optimal Design of a Supersonic Turbine," AIAA 2000-4860, Jan. 2000.

[7]Wang, S., Fan, H., and Xi, G., "Performance Comparison Study of an Improved Genetic Algorithm Applied to an Aerodynamic Design," *Proceedings of the Second International Symposium on Fluid Machinery and Fluid Engineering*, 2000, pp. 88–95.

[8]Pierret, S., "Three-Dimensional Blade Design by Means of an Artificial Neural Network and Navier–Stokes Solver," von Kármán Inst., VKI Rept. 1997-25, Rhode-St-Genese, Belgium, April 1997.

[9]Huang, S. Y., Miller, L. S., and Steck, J. E., "Exploratory Application of Neural Networks to Airfoil Design," AIAA 94-0501, Jan. 1994.

[10]Burman, J., Gebart, B., and Martensson, H., "Development of a Blade Geometry Definition with Implicit Design Variables," AIAA 2000-0671, Jan. 2000.

[11]Rai, M. M., and Madavan, N. K., "Improving the Unsteady Aerodynamic Performance of Transonic Turbines Using Neural Networks," AIAA 2000-0169, Jan. 2000.

[12]Madavan, N. K., Rai, M. M., and Huber, F. W., "Neural Net-Based Redesign of Transonic Turbines for Improved Unsteady Aerodynamic Performance," AIAA 99-2522, June 1999.

[13]Shyy, W., Papila, N., Vaidyanathan, R., and Tucker, P. K., "Global Design Optimization for Aerodynamics and Rocket Propulsion Components," *Progress in Aerospace Sciences*, Vol. 37, No. 1, 2001, pp. 59–118.

[14]Shyy, W., Tucker, P. K., and Vaidyanathan, R., "Response Surface and Neural Network Techniques for Rocket Engine Injector Optimization," AIAA Paper 99-2455, June 1999.

[15]Shyy, W., Papila, N., Tucker, P. K., Vaidyanathan, R., and Griffin, L., "Global Design Optimization for Fluid Machinery Applications," *Proceeding of the Second International Symposium on Fluid Machinery and Fluid Engineering*, 2000, pp. 1–10.

[16]Sobieszczanski-Sobieski, J., and Haftka, R. T., "Multidisciplinary Aerospace Design Optimization: Survey of Recent Developments," *Structural Optimization*, Vol. 14, No. 1, 1997, pp. 1–23.

[17]Papila, N., Shyy, W., Griffin, L., Huber, F., and Tran, K., "Preliminary Design Optimization for a Supersonic Turbine for Rocket Propulsion," AIAA Paper 2000-3242, July 2000.

[18]Myers, R. H., and Montgomery, D. C., *Response Surface Methodology—Process and Product Optimization Using Designed Experiments*, Wiley, New York, 1995, pp. 208–279.

[19]Owen, A., "Orthogonal Arrays for: Computer Experiments, Integration and Visualization," *Statistica Sinica*, Vol. 2, No. 2, 1992, pp. 439–452.

[20]Unal, R., Lepsch, R. A., and McMillin, M. L., "Response Surface Model Building and Multidisciplinary Optimization Using D-Optimal Designs," AIAA Paper 98-4759, Sept. 1998.

[21]Papila, N., Shyy, W., Fitz-Coy, N., and Haftka, R. T., "Assessment of Neural Net and Polynomial-Based Techniques for Aerodynamic Applications," AIAA Paper 99-3167, June 1999.

[22]Madsen, J. I., Shyy, W., and Haftka, R. T, "Response Surface Techniques for Diffuser Shape Optimization," *AIAA Journal*, Vol. 38, No. 9, 2000, pp. 1512–1518.

[23]Tucker, P. K., Shyy, W., and Sloan, J. G., "An Integrated Design/Optimization Methodology for Rocket Engine Injectors," AIAA Paper 98-3513, July 1998.

[24]Rai, M. M., and Madavan, N. K., "Application of Artificial Neural Networks to the Design of Turbomachinery Airfoils," AIAA Paper 1998-1003, Jan. 1998.

[25]Rai, M. M., and Madavan, N. K., "Aerodynamic Design Using Neural Networks," AIAA Paper 98-4928, Aug. 1998.

[26]Vaidyanathan, R., Papila, N., Shyy, W., Tucker, P. K., Griffin, L. W., Fitz-Coy, N., and Haftka, R. T., "Neural Network-Based and Response Surface-Based Optimization Strategies for Rocket Engine Component Design," AIAA Paper 2000-4880, Sept. 2000.

[27]Kosko, B., *Neural Networks and Fuzzy Systems: A Dynamical Systems Approach to Machine Intelligence*, Prentice–Hall, Upper Saddle River, NJ, 1992.

[28]Greenman, R. M., "2-D High-Lift Aerodynamic Optimization Using Neural Networks," NASA TM-1998-112233, June 1998.

[29]Orr, M. J. L., "Matlab Functions for Radial Basis Function Networks," Inst. for Adaptive and Neural Computation Division for Informatics, Edinburgh Univ., Edinburgh, Scotland, U.K., 1999, WEB: http://www.anc.ed.ac.uk/~mjo/rbf.html (03/05/2002).

[30]Orr, M. J. L., "Introduction to Radial Basis Function Networks," Centre for Cognitive Science, Edinburgh Univ., Scotland, U.K., 1996, WEB: http://www.anc.ed.ac.uk/~mjo/rbf.html (03/05/2002).

[31]Orr, M. J. L., "Recent Advances in Radial Basis Function Networks," Technical Rept., Inst. for Adaptive and Neural Computation Division for Informatics, Edinburgh Univ., Scotland, U.K., 1999, WEB: http://www.anc.ed.ac.uk/~mjo/rbf.html (03/05/2002).

[32]"MATLAB: The Language of Technical Computing," Ver. 5.3.0.10183 (R11), MathWorks, Natick, MA, Jan. 1999.

[33]"Statistics and Graphics Guide," JMP Ver. 3, SAS Inst. Inc., Cary, NC, 1998.

[34]Haftka, R. T., Scott, E. P., and Cruz, J. R., "Optimization and Experiments: A Survey," *Applied Mechanics Reviews*, Vol. 51, No. 7, 1998, pp. 435–448.

[35]Microsoft Excel Solver 97, Microsoft Corp., Troy, NY, 1985–1996.

[36]Ladson, L. S., Waren, A. D., Jain, A., and Ratner, M., "Design and Testing of a Generalized Reduced Gradient Code for Nonlinear Programming," *Association for Computing Machinery Transactions on Mathematical Software*, Vol. 4, No. 1, 1978, pp. 51–56.

[37]Griffin, L. W., and Dorney, D. J., "RLV Turbine Performance Optimization," *12th Annual Propulsion Engineering Research Center (PERC) Symposium*, Cleveland, OH, Oct. 2000.

[38]Griffin, L. W., and Dorney, D. J., "Simulations of the Unsteady Flow Through the Fastrac Supersonic Turbine," *Journal of Turbomachinery*, Vol. 122, No. 2, 2000, pp. 225–233.

[39]Griffin, L. W., Dorney, D. J., Huber, F., Shyy, W., Papila, N., and Tran, K., "Detailed Aerodynamic Design Optimization of an RLV Turbine," AIAA Paper 2001-3397, July 2001.

[40]Steffen, C. J., Jr., Smith, T. D., Yungster, S., and Keller, D. J., "Computational Analysis for Rocket-Based Combined-Cycle Systems During Rocket-Only Operation," *Journal of Propulsion and Power*, Vol. 16, No. 6, 2000, pp. 1030–1039.

[41]Burman, J., and Gebart, B. R., "Influence from Numerical Noise in the Objective Function for Flow Design Optimization," *International Journal of Numerical Methods for Heat and Fluid Flow*, Vol. 11, No. 1, 2001, pp. 6–19.